

Geophysical Research Letters

RESEARCH LETTER

10.1029/2019GL086233

Key Points:

- Mesospheric and upper stratospheric initial conditions play an important role in forecasting the onset and development of sudden warmings
- The 5-day lead capture rate of the onset of major sudden stratospheric warmings degrades about 20% if satellite data are not assimilated
- The absence of satellite observations could also affect the extended-range forecast skill related to downward-propagating signals

Supporting Information:

- Supporting Information S1

Correspondence to:

S. Noguchi,
noguchis@jamstec.go.jp

Citation:

Noguchi, S., Kuroda, Y., Mukougawa, H., Mizuta, R., & Kobayashi, C. (2020). Impact of satellite observations on forecasting sudden stratospheric warmings. *Geophysical Research Letters*, 47, e2019GL086233. <https://doi.org/10.1029/2019GL086233>

Received 13 NOV 2019

Accepted 19 FEB 2020

Accepted article online 21 FEB 2020

Impact of Satellite Observations on Forecasting Sudden Stratospheric Warmings

S. Noguchi^{1,2} , Y. Kuroda³ , H. Mukougawa⁴ , R. Mizuta² , and C. Kobayashi² 

¹Research Center for Environmental Modeling and Application, Japan Agency for Marine-Earth Science and Technology, Yokohama, Japan, ²Meteorological Research Institute, Japan Meteorological Agency, Tsukuba, Japan, ³Meteorological College, Japan Meteorological Agency, Kashiwa, Japan, ⁴Graduate School of Science, Kyoto University, Kyoto, Japan

Abstract The observational impacts of satellite data assimilation on extended-range forecasts of sudden stratospheric warmings (SSWs) are investigated by conducting ensemble forecast experiments. We use two Japanese novel reanalysis products: the Japanese 55-year reanalysis (JRA-55) and its subset that assimilates conventional observations only (JRA-55C). A comparative examination on the reproducibility for SSWs between the two ensemble forecasts reveals that the impact of satellite observations is significant for forecasts starting 5 days before the SSW onset, with 20% less accuracy in the JRA-55C forecasts. Moreover, some of forecasts of vortex-splitting SSWs show a sudden appearance of deep difference, which lasts over a few months in the lower stratosphere and significantly affects the surface climate. These results highlight an important role of mesospheric and upper stratospheric circulations on the onset and development of SSWs.

Plain Language Summary Satellite observations are valuable for producing initial conditions for numerical weather prediction (NWP) systems, especially over the upper stratosphere that typical upper-air observations cannot cover. However, many NWP models suffer from biases associated with unresolved processes. This study explores how the NWP system benefited from satellite data in forecasting the breakdown events of stratospheric polar vortices/sudden stratospheric warmings (SSWs) by making many forecasts from typical initial conditions, both with and without satellite data. Due to unresolved bias over the upper stratosphere, some forecasts from no-satellite initial conditions miss the onset of SSWs and subsequent anomalous tropospheric conditions. Thus, the deteriorated grasp of the upper atmosphere in the absence of satellite observations degrades the deterministic predictability of extreme stratospheric events and following downward-propagating signals.

1. Introduction

To improve our understanding and forecasting of the atmospheric environment, it is important to comprehend how analyses and forecasts produced by numerical weather prediction (NWP) systems are affected by each observational source. Observation system experiments (OSEs) examine the impacts of observation on analyses and forecasts (e.g., Bouttier & Kelly, 2001; Zapotocny et al., 2007) but are expensive to run. Moreover, they are executable only in a comprehensive NWP system environment, including sophisticated handling techniques for various observational data. Therefore, many have used a limited number of samples and have been conducted only by operational NWP centers.

In contrast, reanalysis products – produced by NWP systems of constant settings over a long period – are used extensively in climate research and have become so common that many operational centers provide them. The Japan Meteorological Agency provides the Japanese 55-year reanalysis (JRA-55; Kobayashi et al., 2015), which forms the “JRA-55 family” with its subproducts, JRA-55C and JRA-55AMIP. JRA-55C (Kobayashi et al., 2014), whose assimilated data is limited to conventional observations (e.g., land and marine surface data and radiosonde upper-air data), is a temporary homogenized reanalysis particularly suitable for studies of multidecadal variability and climate change. Furthermore, when compared to JRA-55, it can be utilized as OSE data that mainly excludes satellite observations.

Several examinations on the impact of satellite data assimilation have been conducted for sudden stratospheric warming (SSW) events by comparing between JRA-55 and JRA-55C. For example, Noguchi and Kobayashi (2018) reported a failure of JRA-55C in capturing the unique vortex-splitting SSW that

©2020. The Authors.

This is an open access article under the terms of the Creative Commons Attribution License, which permits use, distribution and reproduction in any medium, provided the original work is properly cited.

occurred on September 2002 – the first observed SSW in the Southern Hemisphere. Other recent work suggests there is a small impact of satellite observations on SSW events in the Northern Hemisphere (NH) due to its numerous radiosonde observations, except for the upper stratosphere (e.g., Gerber & Martineau, 2018; Taguchi, 2017). However, they are limited only at the stage of analysis. Based on recent experiments, the onset and development of SSWs depends not only on the wave forcing from the troposphere but also on the state of the stratosphere (e.g., de la Cámara et al., 2017; Noguchi et al., 2016). Consequently, there are active searches for stratospheric signs of the SSW preconditioning (Jucker & Reichler, 2018; Lawrence & Manney, 2020). Therefore, we could expect an exposure of the potential impact of satellite observations at the stage of forecast when NWP integrations are free from the consecutive observational constraints. Furthermore, the difference between JRA-55 and JRA-55C near the model top would reflect deficiencies of gravity wave drag parameterizations and the inevitable damping of atmospheric motions within sponge layers (Noguchi & Kobayashi, 2018). Examining the impact of variability compensated for by assimilating satellite observations (e.g., effects of gravity waves on the basic state) in the time evolution of SSW would therefore be valuable, as possible roles of gravity waves are vigorously discussed in recent studies (Albers & Birner, 2014; Scheffler et al., 2018).

This study investigates the impact of satellite data assimilation on SSW forecasts by conducting and comparing ensemble forecasts using JRA-55 and JRA-55C. To quantify the averaged impact, we conducted forecasts for 20 SSWs in the NH from December to February 1978/1979–2011/2012. The SSW is defined by the zonal-mean zonal wind reversal at 60°N and 10 hPa, and the onset date of SSW (D0) is the date of reversal (Charlton & Polvani, 2007).

2. Experimental Settings

We used an atmospheric general circulation model of the Meteorological Research Institute (MRI-AGCM; e.g., Mizuta et al., 2012) for forecasting, with settings similar to those of Noguchi et al. (2016) and Mukougawa et al. (2017). See Text S1 for details of the model setting. We prepared initial conditions by using the ensemble prediction system of the MRI (MRI-EPS; Yabu et al., 2014). The MRI-EPS generates initial perturbations by a breeding of growing modes method (Toth & Kalnay, 1993). We produced 12 perturbations every day by using JRA-55 as starting data during a breeding of growing modes cycle. By adding and subtracting these perturbations to JRA-55 and JRA-55C, 24 perturbed initial conditions were created beside one control initial condition. Therefore, we have got two equally perturbed 25-member initial conditions every 12 Coordinated Universal Time whose ensemble mean corresponds to JRA-55 and JRA-55C.

We conducted 60-day ensemble forecasts as follows: First, to overview the forecast skill in the usual initial condition, the JRA-55 forecasts are initialized every day from 15 days before the SSW onset date (D–15) to 5 days after that (D+5). Therefore, 21 ensemble forecasts were conducted for each SSW events. Then, five ensemble forecasts starting from JRA-55C were also initialized every 5 days (D–15, –10, –5, 0, +5). By comparing these forecasts from different initial conditions, we can quantify the observational impact of satellite data on SSW forecasts.

3. Results

3.1. Impact on Forecasting the Onset of SSWs

We have examined how accurately ensemble forecasts capture the onset timing of SSW and to what extent it is affected by the assimilation of satellite data (Figure 1). The SSW capture rate is defined as the rate of ensemble members that showed the reversal of the zonal-mean zonal wind at 60°N and 10 hPa during a period of ± 3 days from the JRA-55 SSW central date (D0). For the several events that do not show clear easterly, this binomial judge of SSW onset would be not suitable (e.g., the averaged capture rate does not reach 100% even initialized on D–1). Therefore, we focused here on 12 prominent SSW events (which shows under -10 m s^{-1} easterly within 5 days after the onset date), although this sample squeezing does not affect results for satellite impact (see Figures S1–S3). One can consult the SSW capture rate of individual events in the supplement (Figure S2).

On average, the onset of SSW is predicted deterministically when JRA-55 forecasts are initialized after D–5. Before this, the SSW capture rate decreases immediately, <50% from D–10 and <20% beyond D–15.

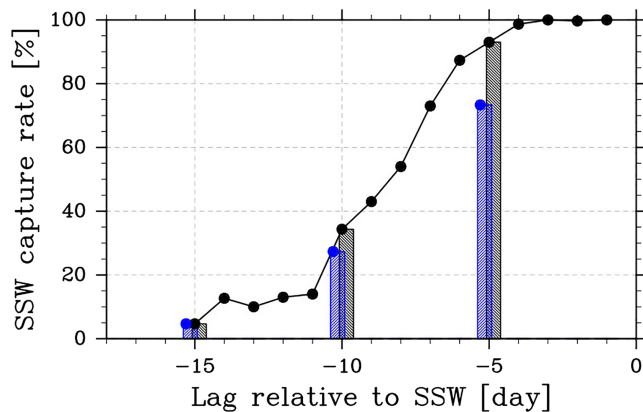


Figure 1. Percentage of ensemble members that predict the reversal of zonal-mean zonal wind within ± 3 days of the onset date of SSW. The capture rate of JRA-55 forecasts starting from D-15 to D-1 for 12 prominent SSW events (black lines with circles). The values of forecasts starting from D-15, D-10, and D-5 are also shown (JRA-55: gray bars, JRA-55C: blue bars).

However, for individual SSW events, the onset of some is captured well even when forecasts are initialized before D-7 (Figure S2). Therefore, the predictability of SSW onset beyond a week depends on individual cases. These results are consistent with previous analyses of operational ensemble forecasts in Taguchi (2016) and Karpechko (2018).

A prominent difference between JRA-55 forecasts and JRA-55C forecasts is a $\sim 20\%$ decrease in the SSW capture rate in the JRA-55C forecast starting from D-5. This difference could reflect the difference in the reanalyses, but there is no difference in the SSW capture rate between the reanalyses for prominent SSWs (i.e., the SSW capture rate of JRA-55C is 100%) according to the current definition of capture rate and targeted SSW events (cf. Taguchi, 2017). Therefore, we conclude that this difference was generated during the numerical prediction from reanalyses. However, it is difficult to find a significant satellite impact on the SSW capture rate in forecasts initialized before that ($\sim 7\%$ in D-10 forecasts at the largest). At lead times beyond a week, the impact from the difference in initial conditions would be obscured by the nonlinear growth of forecast errors. Therefore, it would be hard to detect the impact in terms of the SSW capture rate, especially in the composite of multiple SSWs.

3.2. Impact on Forecasting Circulation Anomalies After SSWs

The impact of satellite observation on forecasting SSWs and following circulation anomalies is examined by using a more general metric of forecast verification – anomaly correlation (AC) for geopotential height fields (Figure 2). The target area is set to the commonly used NH region (north of 20°N), although forecast skills are dominated by those in the polar region (as shown in Figure S4). The practical predictable limit is often estimated as the forecast time when the AC first drops below 0.6 (cf. Kalnay, 2003). Therefore, we could estimate that the predictable period in the troposphere (levels below 100 hPa) is ~ 7 to 9 days; This is consistent with other work (e.g., Ichimaru et al., 2016). On the other hand, the predictable period in the stratosphere is generally longer than that of the troposphere. In particular, the predictable period in the middle stratosphere (~ 10 hPa) is ~ 25 to 27 days if forecasts are initialized after D-5 (Figures 2c-2e). Moreover, a close look at the tropospheric forecast skill for the lead time beyond a week reveals that the AC of forecasts starting from D+5 (Figure 2e) shows a higher value than those from D-15 (Figure 2a). However, this longer predictable period is achieved only after the capture of SSW onset. The AC of forecast starting from D-15 (which failed to capture SSW onset) shows a sudden drop at the onset date of SSW and no skill after that (Figure 2a).

We can see the positive impact ($>10\%$ difference) of including satellite observations, especially in the upper stratosphere before the SSW (Figures 2f-2j). However, the difference is significant only 5-10 days after the initialization. This is a reflection of an initial linear relationship between the improved/degraded initial condition and the improved/degraded forecast that does not hold due to the nonlinear growth of errors. This result is also consistent with the previous result that the satellite impact on the SSW capture rate is largest ($\sim 20\%$) in forecasts starting from D-5. However, for D-5, the impact on stratospheric anomalies after SSW forecasts does not appear in the extended-range forecast period (Figure 2h), although the impact appeared large given the measure of the SSW capture rate. We postulate that this is because the reversal of zonal-mean zonal wind at 10 hPa is not closely linked to the formation of long-lasting anomalies following the SSW.

A positive impact of including satellite observations in the extended forecast period is found in forecasts from D-15 and D-10 but not in those from D-5. The initial conditions of D-15 and D-10 have time to be affected by satellite observations in terms of whether the SSW is captured by forecasts or not, while D-5 is initialized when the formation of anomalies following the SSW is already established. Relatively large improvements in the forecast could be found in the stratosphere after the onset of the SSW in forecasts from D-15 and D-10, although these are disturbed and not judged as significant (Figures 2f and 2g). This suggests that the initial difference in the upper stratosphere, which was induced by satellite data assimilation, would develop due to large anomalies via nonlinear interactions between waves and the mean flow for

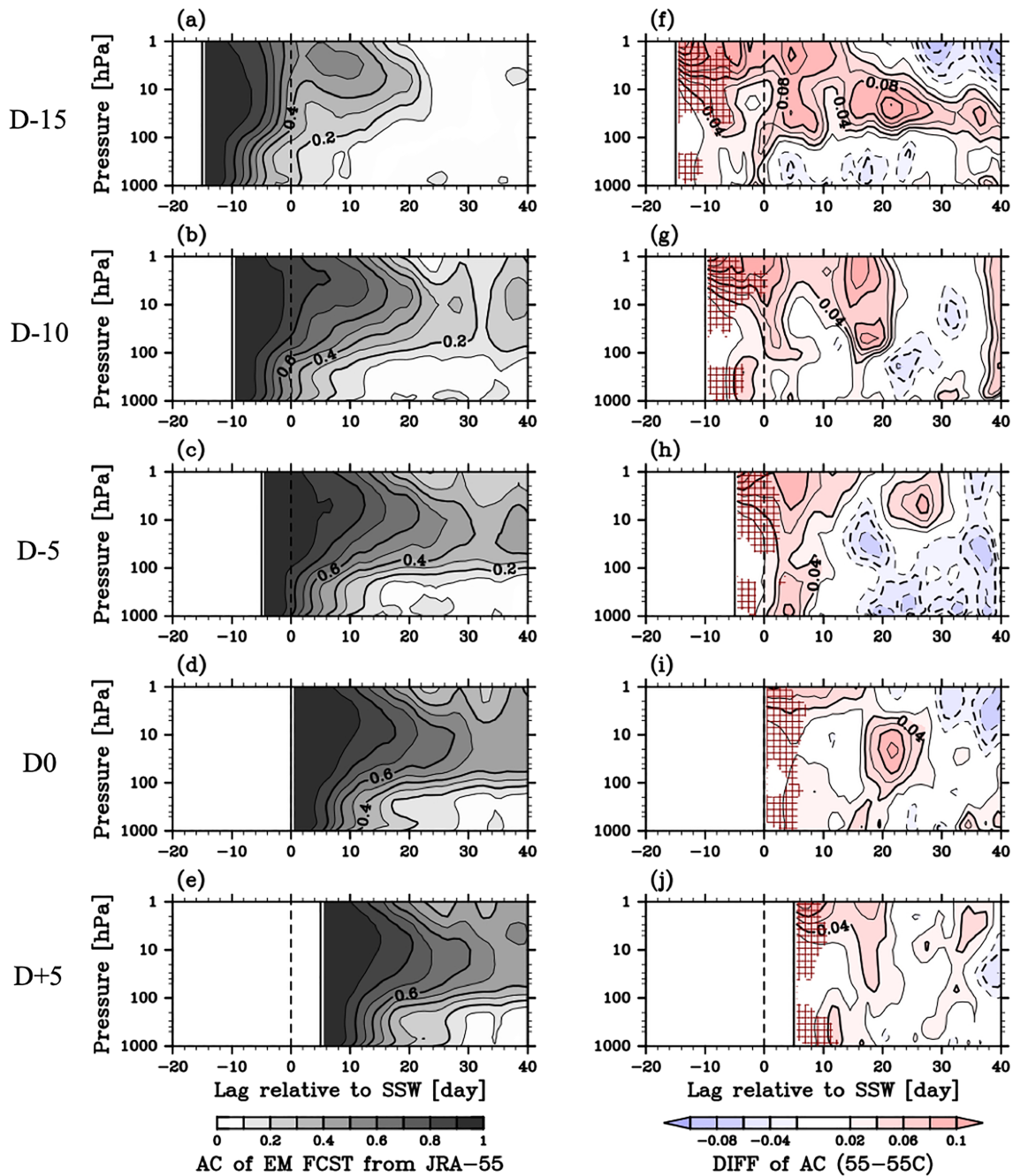


Figure 2. Time-height cross sections of the forecast skill measured by AC coefficient (validated by JRA-55) for geopotential height fields in the NH (north of 20°N). Forecast results from D–15, D–10, D–5, D0, D+5 are distributed from top to bottom. D0 is represented by a vertical broken line. (a)–(e) Composite AC coefficient of ensemble mean JRA-55 forecasts averaged for all (20) SSWs. (f)–(j) Differences of averaged AC coefficient of ensemble mean JRA-55 forecasts from those of JRA-55C forecasts. The hatched regions are where the difference is significant at 90% confidence (estimated by Welch’s *t*-test).

only a small number of SSW events. Therefore, to describe details of the growth process of satellite impact, it is necessary to focus on cases showing a large difference between JRA-55 and JRA-55C forecasts.

3.3. Details of the Impact in an Extreme Case

Details of the initial growth of differences between JRA-55 and JRA-55C forecasts are examined by focusing on a forecast case that had a significant impact due to satellite data assimilation in the extended-range

forecast. We checked the absolute difference of the normalized polar-cap (north of 60°N) height anomalies (a proxy of the NH annular mode; cf, Baldwin & Thompson, 2009) expressed for each initialization timing (see Figure S5). By considering the ensemble-averaged differences in the lower stratosphere (at 50 hPa level) for approximately one month after SSWs (from 5 to 35 days after D0), we chose a forecast case for an SSW event that occurred on 1 January 1985, starting from D−10 as the most prominent example of the satellite impact (Figure S5, red cross). In this case, the deep difference (which reaches the polar troposphere and significantly affects the surface climate) suddenly appears around D0 from the upper stratosphere and lasts in the lower stratosphere for over a few months after SSW (see Figure S6). Other cases of large satellite impact on forecasts from D−15 and D−10 also show persistent lower stratospheric difference after the initial upper stratospheric difference (see Figures S7–S9). Note that their signs of difference are the same that the JRA-55 forecast shows a higher polar-cap height anomaly, although opposite-sign cases are also possible, especially as the onset date of SSW getting closer (Figure S10).

Time evolutions of key parameters in the forecasts in this case describe how the JRA-55 and JRA-55C forecasts compare (Figure 3). A failure to capture the sudden warming in the JRA-55C forecast is clear (Figure 3a). The JRA-55 ensemble forecast captures well the onset of warming (over 25 K) whose peak is in early January. However, the warming in the JRA-55C forecast is weakened after 26 December, and its peak value stays ~15 K lower than those of JRA-55, although JRA-55C follows JRA-55 well (with a difference of <5 K).

Differences in predicted stratospheric circulations are recognizable in the geometric shape of the stratospheric polar vortex around 29 December when the discrepancy between forecasts becomes crucial (Figure 3c). The polar vortex in the JRA-55 forecast splits into two pieces with an almost barotropic structure throughout the stratosphere, while the JRA-55C forecast holds its shape as a single vortex strained parallel to the direction between Eurasia and North America. As a result, the deep difference reaching to the lower stratosphere (and even to the troposphere) appears suddenly around the SSW onset date and lasts for over a month.

To investigate the initial trigger that leads to different time evolutions in the forecasts, we have shown the state of the wave-mean flow interactions just after the initialization in both forecasts (Figure 4). From 23–25 December, the Eliassen-Palm (E-P) flux (Andrews et al., 1987) in the lower stratosphere begins to increase (Figure 3b), and there is a strong convergence of E-P flux at 50–60°N and 1 hPa in the JRA-55 forecast (Figure 4a). This convergence is synonymous with the amplification of wave components in the upper stratosphere, especially zonal wavenumber 2 – the initiation of the splitting behavior of the polar vortex. In contrast, the upward-propagating wave activity is refracted more equatorward, and the convergence of E-P flux is absent in the JRA-55C forecast, alternatively generated at 30–40°N (Figure 4b). Such difference is caused by a too strong westerly (zonal-mean) wind field in the initial condition particularly over the upper stratosphere. The JRA-55C suffers from a strong wind bias of the polar-night jet (“cold pole biases”; MRI-AGCM also has a similar bias as shown in Figure S11) near the model top that is partly solved by the inclusion of satellite observations in JRA-55. This changes the wave propagation property in the stratosphere and prevents the convergence at the correct location, as shown in the significant difference between the JRA-55 and JRA-55C forecasts (Figure 4c). The initial triggering process starts from the region above the upper stratosphere, since there is almost no significant difference in the wave activity flux in the troposphere during this period.

After the appearance of the initial changes in the wave propagation property in the upper stratosphere, further changes are seen in the time series of the E-P flux in the lower stratosphere (Figure 3b). After 27 December, the upward wave activity in the JRA-55 forecast continues to grow through positive feedback by the wave amplification (i.e., the deceleration of westerly zonal-mean wind) and further upward propagation of the wave activity in the preferable mean-field. In contrast, the growth of the flux slows down in the JRA-55C forecast due to the absence of the wave amplification in the upper stratosphere. As a result, the difference is expanded until the peak of the flux in the JRA-55 forecast. Such a control of the upward flux from the troposphere by the stratospheric circulation is sometimes demonstrated by mechanistic circulation models (Hitchcock & Haynes, 2016; Scott & Polvani, 2004, 2006). In this study, we have found an example of the stratospheric control of the following wave activity flux in a sophisticated AGCM forecast experiment that is conducted as the OSE of satellite observations.

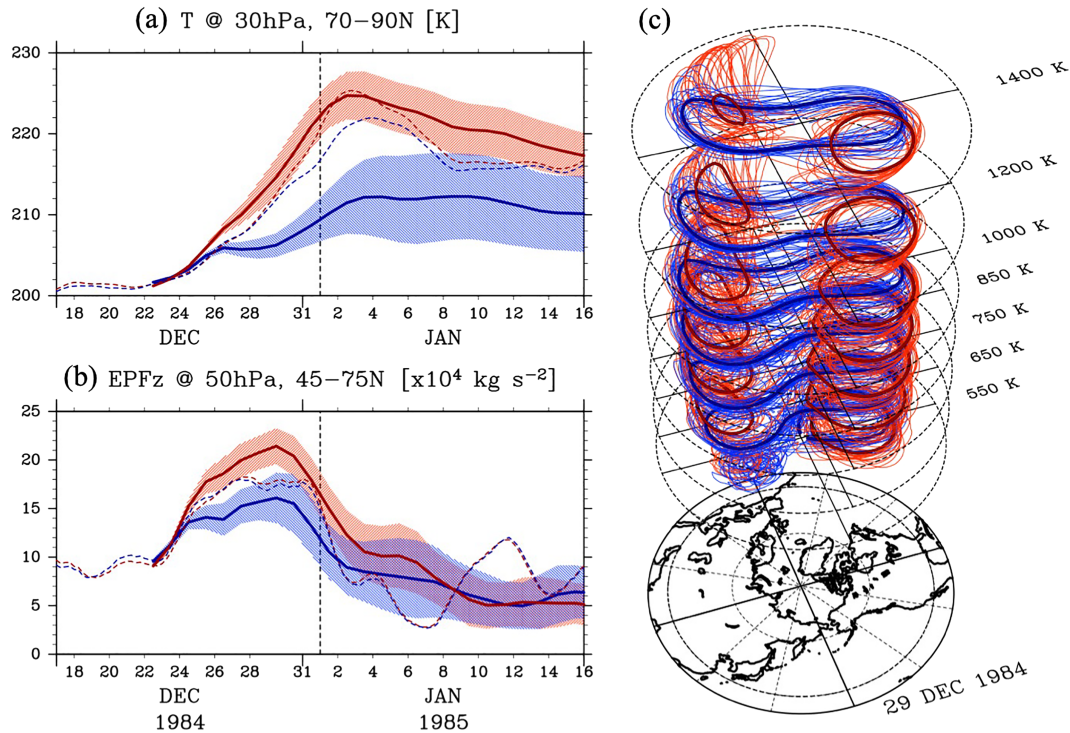


Figure 3. Satellite impact on forecasts of SSW onset in an extreme case. JRA-55 (red line) and JRA-55C (blue line) ensemble forecasts starting from D-10 are shown for an SSW that occurred on 1 January 1985. Time series of (a) 30-hPa temperature averaged northward of 70°N and (b) vertical component of 50-hPa E-P flux that averaged over 45–75°N. Thick lines and shades indicate the ensemble mean values and 0.5 standard deviations among ensemble members. JRA-55 and JRA-55C are also shown by dotted lines. (c) Three-dimensional distributions of the vortex edges (isolines of the vertically weighted potential vorticity), of the stratospheric polar vortex, for a 7-day forecast field (validated at 3 days before D0). As a vortex edge, 38 PVU contours of Lait’s PV at isothermal surfaces are plotted for each ensemble forecasts (cf. Matthewman et al. 2009). Thick lines indicate the ensemble means.

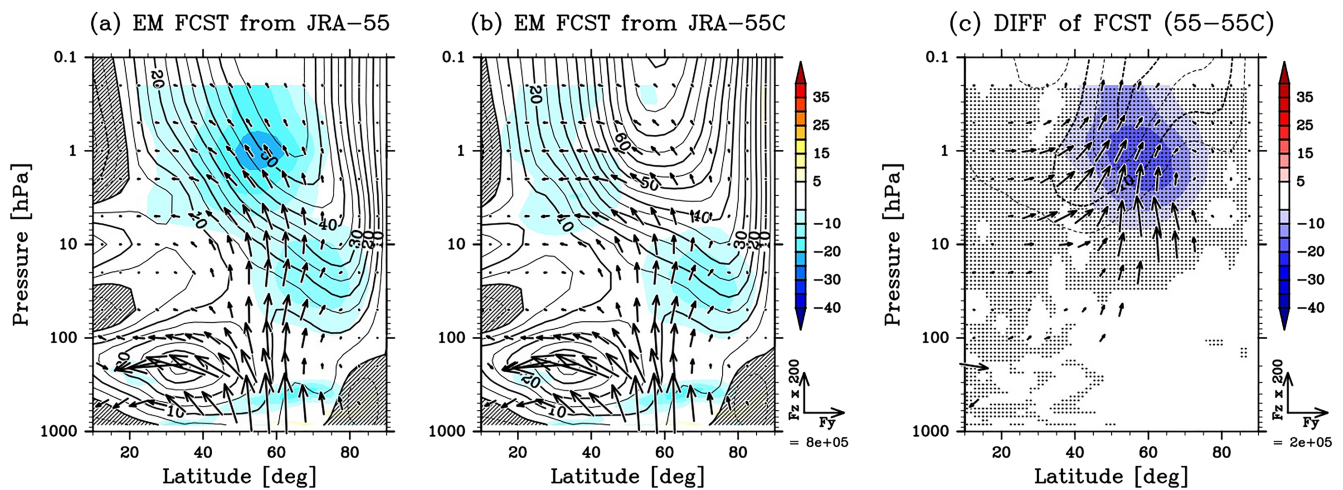


Figure 4. Latitude-height cross sections before SSW (occurred on 1 January 1985) in an extreme case of satellite impact. Ensemble mean forecasts starting from D-10 fields of (a) JRA-55 and (b) JRA-55C averaged over the initial 1–3 days (7–9 days before D0) are shown as zonal-mean zonal wind (contours with an interval of 5 m s^{-1}), E-P flux vector scaled by the inverse of the square root of the pressure (arrows: $\text{Pa}^{-0.5} \text{ kg s}^{-2}$), and its divergence (color: $\text{m s}^{-1} \text{ day}^{-1}$). The region of easterly is shaded. (c) Difference between them [(a) – (b)]. The regions where the difference of E-P flux divergence is significant at 90% confidence (estimated by Welch’s *t*-test) are hatched. The significant (>90% in both meridional and vertical) differences of E-P flux are also plotted by four times large vectors.

4. Summary and Discussion

We have examined observational impacts of satellite data assimilation on extended-range forecasts of SSWs by conducting ensemble forecast experiments for 20 SSW events using JRA-55 and JRA-55C combined with the flexible ensemble forecast system “MRI-EPS.”

We have demonstrated the satellite impact on forecasts of the SSW onset judged by the current de facto standard measure of the major SSW: the reversal of the zonal-mean zonal wind at 60°N and 10 hPa. A comparative examination between the two ensemble forecasts revealed that the difference in the SSW capture rate is largest for forecasts starting 5 days before the SSW onset, on average. The SSW capture rate in JRA-55C forecasts is about 20% lower than that of JRA-55 forecasts, which correctly capture the onset timing of SSWs (allowing ± 3 days difference). The lead 5 days is within the deterministic predictable limit as shown in our forecast experiment starting from every day in JRA-55 fields. The predictable period of SSW onset is reported more than 5 days in many previous studies (cf. Tripathi et al., 2015). This result suggests that a current practical agreement of the deterministic limit of SSW predictability (at least 5 days) owes to the quality of the initial condition that benefits from the use of satellite information. Therefore, the lack of satellite data for any reason might lead to a serious degradation in the lower (strict) limit of the prior grasp of the event onset that is important for real-time warnings.

We have also shown that the satellite impact on forecasts of circulation anomalies after SSWs, which are expected as a source of predictability in the seasonal forecasts. On average, we see >10% improvement due to satellite observations in the AC coefficients of the forecasted NH height fields, especially in the upper stratosphere. Such difference in the forecast skill is significant only before 5–10 days after the initialization since the forecast errors grow nonlinearly and the relative contribution of the initial conditions becomes small after that. However, there are some extreme cases of long-lasting impact at the lower stratosphere, depending on whether deep anomalies associated with SSWs are well captured or not in forecasts starting from more than 10 days before the SSW onset date. Such a case dependency is not unexpected considering that not all SSWs are followed by long-lasting anomalies, and not all SSWs are sensitive to the analysis increments (mainly over the upper stratosphere) induced by the satellite data assimilation.

Finally, details of the satellite impact that eventually affects the extended-range forecast are described by focusing on an extreme case. Due to the absence of observational corrections near the model top, the convergence of E-P flux in the upper stratosphere just after the initialization is prevented by a too strong westerly mean-wind field (i.e., the uncured bias of the NWP model of JRA-55) in the JRA-55C forecast. This leads to reduced positive feedbacks between upward wave fluxes and the mean-field and consequently, unlike the JRA-55 forecast, the JRA-55C forecast failed to reproduce the splitting behavior of the stratospheric polar vortex. This causes a deep difference between both forecasts that reaches to the lower stratosphere (and the surface) and lasts over a month after the SSW. Since the polar vortex just before the splitting is considered to be located near a critical point in the phase space (e.g., Matthewman & Esler, 2011; Yasuda et al., 2017), a transition between states could be caused even by minute differences. Thus, variations compensated by satellite data assimilation, which represents the effects of incompletely resolved processes of the NWP model (e.g., gravity wave drags for the mean flow), are possible candidates triggering such phase transitions. By introducing stochastic noise to a schematic model of SSW, Birner and Williams (2008) claimed that such small forcing (mimicking the effects of gravity waves) could affect a threshold of the SSW-like phase transition. The bifurcating behavior in the extreme case of this study might be an equivalent representation in the real atmosphere. Considering the claim of recent studies that only 20% of all anomalous tropospheric wave events are followed by SSW-like events (Birner & Albers, 2017; de la Cámara et al., 2019), contributions of such a positive feedback process would not be small.

These results highlight the important role of mesospheric and upper stratospheric circulations on the onset and development of SSWs, and in this paper, we have confirmed the impact of satellite data assimilation on the reproducibility of SSWs. In particular, those that occur in the NH, whose time evolutions are more constrained by abundant conventional observations compared with those of the Southern Hemisphere. Note that changes in the observation system (see Text S2 for one example) cast a challenge in our ability to grasp the atmospheric environment. Further studies are needed in order to reveal potential changes in SSW reproducibility depending on various changes in the observation system.

Acknowledgments

This work was partly supported by Grants-in-Aid for Scientific Research (16J09665, 19K14798) from the Japan Society for the Promotion of Science. The JRA-55 family data sets are available on the JMA Data Dissemination System (http://jra.kishou.go.jp/JRA-55/index_en.html) and collaborative organizations (detailed information is available on the JRA-55 website). The numerical data used in this study are available (<https://doi.org/10.5281/zenodo.3538978>). The GFD-DENNOU Library was used for graphics. We thank two anonymous reviewers for their constructive comments.

References

Albers, J. R., & Birner, T. (2014). Vortex preconditioning due to planetary and gravity waves prior to sudden stratospheric warmings. *Journal of the Atmospheric Sciences*, *71*, 4028–4054. <https://doi.org/10.1175/JAS-D-14-0026.1>

Andrews, D., Holton, J., & Leovy, C. (1987). *Middle atmosphere dynamics* (p. 489). San Diego: Academic Press Inc.

Baldwin, M. P., & Thompson, D. W. J. (2009). A critical comparison of stratosphere–troposphere coupling indices. *Quarterly Journal of the Royal Meteorological Society: A journal of the atmospheric sciences, applied meteorology and physical oceanography*, *135*, 1661–1672. <https://doi.org/10.1002/qj.479>

Birner, T., & Albers, J. R. (2017). Sudden stratospheric warmings and anomalous upward wave activity flux. *SOLA*, *13A*, 8–12. <https://doi.org/10.2151/sola.13A-002>

Birner, T., & Williams, P. D. (2008). Sudden stratospheric warmings as noise-induced transitions. *Journal of the Atmospheric Sciences*, *65*(10), 3337–3343. <https://doi.org/10.1175/2008JAS2770.1>

Bouttier, F., & Kelly, G. (2001). Observing-system experiments in the ECMWF 4D-Var data assimilation system. *Quarterly Journal of the Royal Meteorological Society*, *127*, 1469–1488. <https://doi.org/10.1002/qj.49712757419>

Charlton, A. J., & Polvani, L. M. (2007). A new look at stratospheric sudden warmings. Part I: Climatology and modeling benchmarks. *Journal of Climate*, *20*(3), 449–469. <https://doi.org/10.1175/JCLI3996.1>

de la Cámara, A., Albers, J. R., Birner, T., Garcia, R. R., Hitchcock, P., Kinnison, D. E., & Smith, A. K. (2017). Sensitivity of sudden stratospheric warmings to previous stratospheric conditions. *Journal of the Atmospheric Sciences*, *74*, 2857–2877. <https://doi.org/10.1175/JAS-D-17-0136.1>

de la Cámara, A., Birner, R., & Albers, J. R. (2019). Are sudden stratospheric warmings preceded by anomalous tropospheric wave activity? *Journal of Climate*, *32*, 7173–7189. <https://doi.org/10.1175/JCLI-D-19-0269.1>

Gerber, E. P., & Martineau, P. (2018). Quantifying the variability of the annular modes: Reanalysis uncertainty vs. sampling uncertainty. *Atmospheric Chemistry and Physics*, *18*, 17,099–17,117. <https://doi.org/10.5194/acp-18-17099-2018>

Hitchcock, P., & Haynes, P. (2016). Stratospheric control of planetary waves. *Geophysical Research Letters*, *43*, 11,884–11,892. <https://doi.org/10.1002/2016GL071372>

Ichimaru, T., Noguchi, S., Hirooka, T., & Mukougawa, H. (2016). Predictability changes of stratospheric circulations in northern hemisphere winter. *Journal of the Meteorological Society of Japan. Ser. II*, *94*, 7–24. <https://doi.org/10.2151/jmsj.2016-001>

Jucker, M., & Reichler, T. (2018). Dynamical precursors for statistical prediction of stratospheric sudden warming events. *Geophysical Research Letters*, *45*, 13,124–13,132. <https://doi.org/10.1029/2018GL080691>

Kalnay, E. (2003). *Atmospheric modeling, data assimilation and predictability* (p. 341). Cambridge, UK: Cambridge University Press.

Karpechko, A. Y. (2018). Predictability of sudden stratospheric warmings in the ECMWF extended-range forecast system. *Monthly Weather Review*, *146*(4), 1063–1075. <https://doi.org/10.1175/MWR-D-17-0317.1>

Kobayashi, C., Endo, H., Ota, Y., Kobayashi, S., Onoda, H., Harada, Y., et al. (2014). Preliminary results of the JRA-55C, an atmospheric reanalysis assimilating conventional observations only. *SOLA*, *10*, 78–82. <https://doi.org/10.2151/sola.2014-016>

Kobayashi, S., Ota, Y., Harada, Y., Ebata, A., Moriya, M., Onoda, H., et al. (2015). The JRA-55 reanalysis: General specifications and basic characteristics. *Journal of the Meteorological Society of Japan. Ser. II*, *93*(1), 5–48. <https://doi.org/10.2151/jmsj.2015-001>

Lawrence, Z. D., & Manney, G. L. (2020). Does the Arctic stratospheric polar vortex exhibit signs of preconditioning prior to sudden stratospheric warmings? *Journal of the Atmospheric Sciences*, *77*, 611–632. <https://doi.org/10.1175/JAS-D-19-0168.1>

Matthewman, N. J., & Esler, J. G. (2011). Stratospheric sudden warmings as self-tuning resonances. Part I: Vortex splitting events. *Journal of the Atmospheric Sciences*, *68*(11), 2481–2504. <https://doi.org/10.1175/JAS-D-11-07.1>

Matthewman, N. J., Esler, J. G., Charlton-Perez, A., & Polvani, L. M. (2009). A new look at stratospheric sudden warmings. Part III: Polar vortex evolution and vertical structure. *Journal of Climate*, *22*(6), 1566–1585. <https://doi.org/10.1175/2008JCLI2365.1>

Mizuta, R., Yoshimura, H., Murakami, H., Matsueda, M., Endo, H., Ose, T., et al. (2012). Climate simulations using MRI-AGCM3.2 with 20-km grid. *Journal of the Meteorological Society of Japan*, *90A*, 233–258. <https://doi.org/10.2151/jmsj.2012-A12>

Mukougawa, H., Noguchi, S., Kuroda, Y., Mizuta, R., & Kodera, K. (2017). Dynamics and predictability of downward-propagating stratospheric planetary waves observed in March 2007. *Journal of the Atmospheric Sciences*, *74*(11), 3533–3550. <https://doi.org/10.1175/JAS-D-16-0330.1>

Noguchi, S., & Kobayashi, C. (2018). On the reproducibility of the September 2002 vortex splitting event in the Antarctic stratosphere achieved without satellite observations. *Quarterly Journal of the Royal Meteorological Society*, *144*, 184–194. <https://doi.org/10.1002/qj.3193>

Noguchi, S., Mukougawa, H., Kuroda, Y., Mizuta, R., Yabu, S., & Yoshimura, H. (2016). Predictability of the stratospheric polar vortex breakdown: An ensemble reforecast experiment for the splitting event in January 2009. *Journal of Geophysical Research: Atmospheres*, *121*, 3388–3404. <https://doi.org/10.1002/2015JD024581>

Scheffler, G., Pulido, M., & Rodas, C. (2018). The role of gravity wave drag optimization in the splitting of the Antarctic vortex in the 2002 sudden stratospheric warming. *Geophysical Research Letters*, *45*, 6719–6725. <https://doi.org/10.1029/2018GL077993>

Scott, R. K., & Polvani, L. M. (2004). Stratospheric control of upward wave flux near the tropopause. *Geophysical Research Letters*, *31*, L02115. <https://doi.org/10.1029/2003GL017965>

Scott, R. K., & Polvani, L. M. (2006). Internal variability of the winter stratosphere. Part I: Time-independent forcing. *Journal of the Atmospheric Sciences*, *63*, 2758–2776. <https://doi.org/10.1175/JAS3797.1>

Taguchi, M. (2016). Predictability of major stratospheric sudden warmings: Analysis results from JMA operational 1-month ensemble predictions from 2001/02 to 2012/13. *Journal of the Atmospheric Sciences*, *73*, 789–806. <https://doi.org/10.1175/JAS-D-15-0201.1>

Taguchi, M. (2017). Comparison of large-scale dynamical variability in the extratropical stratosphere among the JRA-55 family data sets: Impacts of assimilation of observational data in JRA-55 reanalysis data. *Atmospheric Chemistry & Physics*, *17*, 11,193–11,207. <https://doi.org/10.5194/acp-17-11193-2017>

Toth, Z., & Kalnay, E. (1993). Ensemble forecasting at NMC: The generation of perturbations. *Bulletin of the American Meteorological Society*, *74*(12), 2317–2330. [https://doi.org/10.1175/1520-0477\(1993\)074<2317:EFANTG>2.0.CO;2](https://doi.org/10.1175/1520-0477(1993)074<2317:EFANTG>2.0.CO;2)

Tripathi, O. P., Baldwin, M., Charlton-Perez, A., Charron, M., Eckermann, S. D., Gerber, E., et al. (2015). The predictability of the extratropical stratosphere on monthly time-scales and its impact on the skill of tropospheric forecasts. *Quarterly Journal of the Royal Meteorological Society*, *141*, 987–1003. <https://doi.org/10.1002/qj.2432>

Yabu, S., Mizuta, R., Yoshimura, H., Kuroda, Y., & Mukougawa, H. (2014). Meteorological Research Institute Ensemble Prediction System (MRI-EPS) for climate research. *Technical Report Meteorological Research Institute*, *71*, 63.

- Yasuda, Y., Bouchet, F., & Venaille, A. (2017). A new interpretation of vortex-split sudden stratospheric warmings in terms of equilibrium statistical mechanics. *Journal of the Atmospheric Sciences*, *74*(12), 3915–3936. <https://doi.org/10.1175/JAS-D-17-0045.1>
- Zapotocny, T. H., Jung, J. A., Le Marshall, J. F., & Treadon, R. E. (2007). A two-season impact study of satellite and in situ data in the NCEP Global Data Assimilation System. *Weather and Forecasting*, *22*(4), 887–909. <https://doi.org/10.1175/WAF1025.1>

References From the Supporting Information

- Ebita, A., Kobayashi, S., Ota, Y., Moriya, M., Kumabe, R., Onogi, K., et al. (2011). The Japanese 55-year reanalysis “JRA-55”: An interim report. *SOLA*, *7*, 149–152. <https://doi.org/10.2151/sola.2011-038>
- Fujiwara, M., Wright, J. S., Manney, G. L., Gray, L. J., Anstey, J., Birner, T., et al. (2017). Introduction to the SPARC Reanalysis Intercomparison Project (S-RIP) and overview of the reanalysis systems. *Atmospheric Chemistry and Physics*, *17*, 1417–1452. <https://doi.org/10.5194/acp-17-1417-2017>
- Iwasaki, T., Yamada, S., & Tada, K. (1989). A parameterization scheme of orographic gravity wave drag with two different vertical partitionings. Part I: Impacts on medium-range forecasts. *Journal of the Meteorological Society of Japan. Ser. II.*, *67*, 11–27. https://doi.org/10.2151/jmsj1965.67.1_11
- Tripathi, O. P., Baldwin, M., Charlton-Perez, A., Charron, M., Cheung, J. C., Eckermann, S. D., et al. (2016). Examining the predictability of the stratospheric sudden warming of January 2013 using multiple NWP systems. *Monthly Weather Review*, *144*(5), 1935–1960. <https://doi.org/10.1175/MWR-D-15-0010.1>